7874 *J. Med. Chem.* **2010,** *53,* 7874–7878
DOI: 10.1021/jm1007566

Journal of Medicinal Chemistry
Brief Article

# Indazolylpyrazolopyrimidine as Highly Potent B-Raf Inhibitors with in Vivo Activity

Xiaolun Wang,*[,†,‡] Dan M. Berger,[†] Edward J. Salaski,[†] Nancy Torres,[†] Minu Dutia,[†] Cilien Hanna,[†] Yongbo Hu,[†] Jeremy I. Levin,[†] Dennis Powell,[†] Donald Wojciechowicz,[†] Karen Collins,[†] Eileen Frommer,[†] and Judy Lucas[†]

[†]*Pfizer Global Research and Development, 401 N. Middletown Road, Pearl River, New York 10965, United States , and*
[‡]*Pfizer Global Research and Development, 200 Cambridgepark Drive, Cambridge, Massachusetts 02140, United States*

*Received June 21, 2010*

Novel indazolylpyrazolo[1,5-*a*]pyrimidine analogues have been prepared and found to be extremely potent type I B-Raf inhibitors. The lead compound shows good selectivity against a panel of 60 kinases, possesses a desirable pharmacokinetic profile, and demonstrates excellent in vivo antitumor efficacy in B-Raf mutant xenograft models.

## Introduction

The Ras-Raf-MEK[a]-ERK signal transduction pathway is critical for cell survival, growth and proliferation.[1] One of the key components in this cascade, B-Raf, when mutated (B-Raf$^{V600E}$) plays an important role in the development of cancer.[2] Thus, inhibition of mutant B-Raf offers a viable means for treating cancer.[3] Recently we disclosed a series of type I pyrazolopyrimidine B-Raf inhibitors[4] including **1a** (Figure 1) having an indazole as phenol replacement. While **1a** exhibits much better microsomal stability than the corresponding phenol analogue **1b**, its cell potency against A375 bearing B-Raf$^{V600E}$ is moderate. Therefore, further optimization for the indazolylpyrazolopyrimidine series was initiated, which eventually led to the discovery of compounds with excellent antitumor efficacy in vivo against tumors driven by the mutant B-Raf.

## Results and Discussion

We started our optimization by exploring the influence of substitutions to the phenyl linker. The synthesis of indazolylpyrazolopyrimidine analogues (Table 1) is exemplified with the preparation of **8l** (Scheme 1). Aromatic nucleophilic substitution of fluoroacetophenone **4l** with commercially available (1*S*,4*S*)-*tert*-butyl-2,5-diazabicyclo[2.2.1]heptane-2-carboxylate followed by reaction with DMA−DMF afforded enaminone **6l**, which was then annulated with aminopyrazole **3**[4] to give **7l**. Deprotection of intermediate **7l** followed by a reductive amination with formaldehyde provided the final product **8l**. As reported previously,[4] the introduction of a small ortho group ($R^1$) resulted in a significant B-Raf potency enhancement (**8a**−**d**) while compounds with large ortho groups such as trifluoromethyl (**8e**) and dimethylamino (**8f**) were deleterious. Substitutions on the meta position (**8g**,**h**) or a large naphthyl linker (**8i**) provided no advantage over the unsubstituted analogue. Interestingly when the diazabicycloheptyl headpiece was moved to the ortho position, the resulting **8o** still retained a moderate activity against B-Raf, while the *m*-diazabicycloheptyl **8p** showed a significant loss of potencies. Mono-/polyfluorination on the various positions of phenyl linker (**8b, g, j**−**n**) was beneficial for enzyme and cell potencies except the meta fluorinated analogue (**8g,m**). An increase of potency was observed when a fluorine atom is introduced in the 7 position of the indazole ring (**8q**−**t**), which is consistent with the SAR of the phenol series.[4] It was found that **8l** possessing two ortho fluorine atoms stood out with $IC_{50}$ of 0.16 and 24 nM against B-Raf and A375 cell line, respectively.

A binding model of **8l** with active conformation B-Raf was constructed (Figure 2).[5] Compound **8l** is well accommodated in the ATP-binding pocket, and a key hydrogen bond is formed between the pyridyl nitrogen atom and Cys532 in the hinge range. The indazole moiety behaves as a hydrogen bond donor to Glu501 and a hydrogen bond acceptor from Asp594, mimicking well the phenol binding mode.[6] One fluorine atom occupies a small hydrophobic pocket defined by Ile463, Gly464, and Val471, which explains the potency enhancement brought by a small substituent ortho to the pyrazolopyrimidine core. The second fluorine atom does not appear to have a corresponding lipophilic pocket but may help to avoid entropy loss upon complexation. The diazabicyclo[2.2.1]heptyl group is partially solvent exposed. Therefore, variation in the heterobicyclic moiety might be a viable approach for better physicochemical properties. Another binding model was also built for **8o** with an ortho **A1** substituent (Figure 3). The phenyl linker of **8o** is moved to the bottom of the pocket, and a hydrogen bond between the protonated aliphatic amine and Ser465 in the G-loop is recognized. This new binding mode may be relevant to the single digit B-Raf $IC_{50}$ of **8o**, though the protein has to make some movement to accommodate the bulky ortho substituent.

From our early work,[4] we found that the diazabicyclo[2.2.1]heptyl headpiece is superior to other diazabicyclic groups tested. To further investigate the headpiece SAR especially for the cell activity, we examined several new substituents (Table 2). Compounds **15a** and **15b** were prepared by a similar route used for lead **1a**.[4] The preparation (Scheme 2)

*To whom correspondence should be addressed. Phone: 617-665-5212. Fax: 617-665-5682. E-mail: xxw104@gmail.com.

[a] Abbreviations: MAPK, mitogen-activated protein kinase; ERK, extracellular signal-regulated kinase; MEK, mitogen-activated protein kinase; SAR, structure−activity relationship.

 Published on Web 10/20/2010 

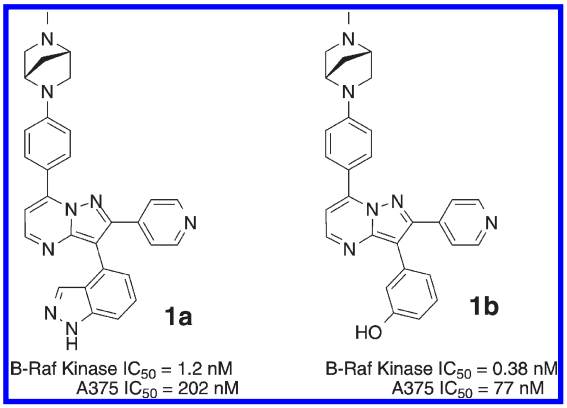


**Figure 1.** Indazolylpyrazolopyrimidine lead **1**.

**Table 1.** Phenyl Linker Modifications of Indazolylpyrazolopyrimidines

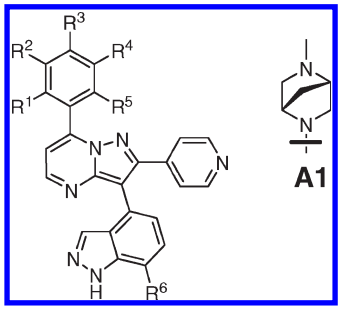


| compd | $R^1$ | $R^2$ | $R^3$ | $R^4$ | $R^5$ | $R^6$ | B-Raf $IC_{50}$ (nM) | A375 cell $IC_{50}$ ($\mu$M) |
|---|---|---|---|---|---|---|---|---|
| **8a** | Me | | **A1** | | | | 0.51 | 0.137 |
| **8b** | F | | **A1** | | | | 0.23 | 0.044 |
| **8c** | Cl | | **A1** | | | | < 0.10 | 0.039 |
| **8d** | Br | | **A1** | | | | < 0.32 | nd |
| **8e** | $CF_3$ | | **A1** | | | | 1.4 | nd |
| **8f** | $NMe_2$ | | **A1** | | | | 7.3 | 1.851 |
| **8g** | | F | **A1** | | | | 1.9 | nd |
| **8h** | | $CF_3$ | **A1** | | | | 2.0 | 0.273 |
| **8i** | Naphthyl | | **A1** | | | | 1.0 | 25 |
| **8j** | F | F | **A1** | | | | 0.61 | 0.107 |
| **8k** | F | | **A1** | F | | | 0.38 | 0.087 |
| **8l** | F | | **A1** | | F | | 0.16 | 0.024 |
| **8m** | | F | **A1** | F | | | 9.6 | 1.253 |
| **8n** | F | F | **A1** | F | F | | 0.35 | 0.070 |
| **8o** | **A1** | | F | | | | 1.4 | 0.250 |
| **8p** | | **A1** | | | | | 61 | 1.397 |
| **8q** | | | **A1** | | | F | 0.50 | 0.068 |
| **8r** | Me | | **A1** | | | F | < 0.32 | 0.188 |
| **8s** | F | | **A1** | | | F | < 0.1 | 0.033 |
| **8t** | F | | **A1** | | F | F | 0.11 | 0.017 |

of analogues **15c–g** started with an annulation between aminopyrazole **3** and diethyl ethoxymethylenemalonate (**9**) followed by a saponification to give carboxylic acid **12**. Decarboxylation and then chlorination of intermediate **12** gave chloropyrazolopyrimidine **13**. Suzuki coupling of intermediate **13** with boronic acid **10** followed by a reductive amination provided the final products (**15c–g**). Compounds **15a** and **15b** with a two-carbon bridge exhibited similar enzyme activity as the corresponding diazabicyclo[2.2.1]heptyl analogues but were less potent in the cell assay. Other heterobicyclic headpieces (**15c–g**) were also detrimental to the cell potency.

The kinase selectivity profile of **8l** was evaluated against a panel of 60 protein kinases.[7] Only 10 kinases including B-Raf and C-Raf showed higher than 70% activity inhibition at 1 $\mu$M **8l**. Compound **8l** exhibits greater than 340-fold selectivity for non-Raf kinases, and the selectivity for C-Raf ($IC_{50}$ = 8.5 nM) is 30-fold. The high selectivity of **8l** minimizes the possibility of any undesired off-target effects.

**Scheme 1**[a]

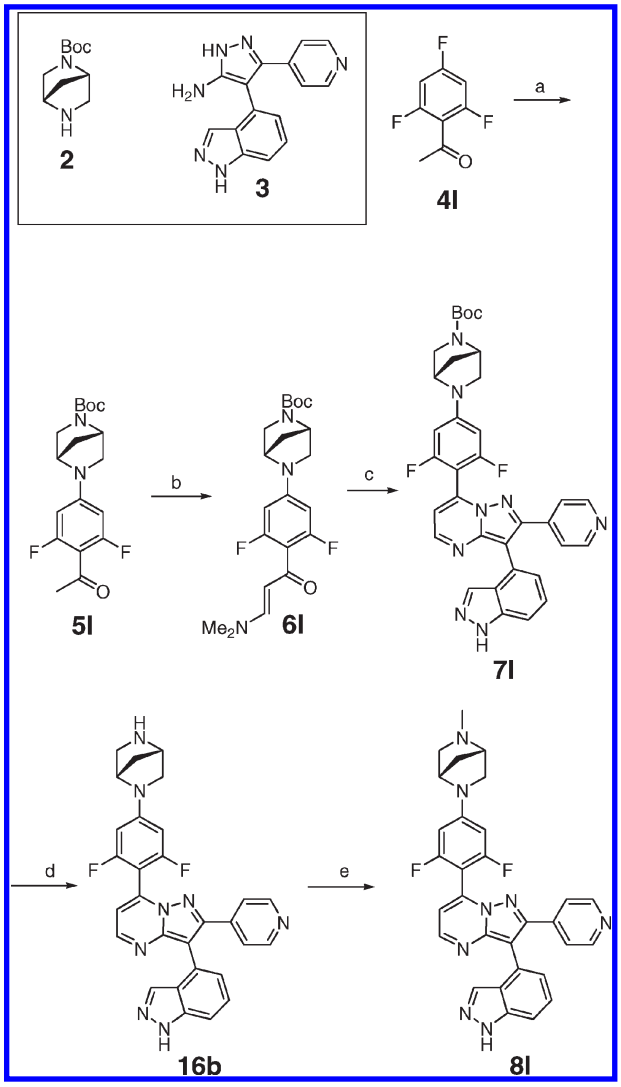


[a] (a) **2**, $K_2CO_3$, HMPA, 62%; (b) DMF–DMA, reflux, 90%; (c) TFA, methanol, 87%; (d) 6 N HCl, 92%; (e) HCHO, $NaBH(OAc)_3$, DMF, 85%.

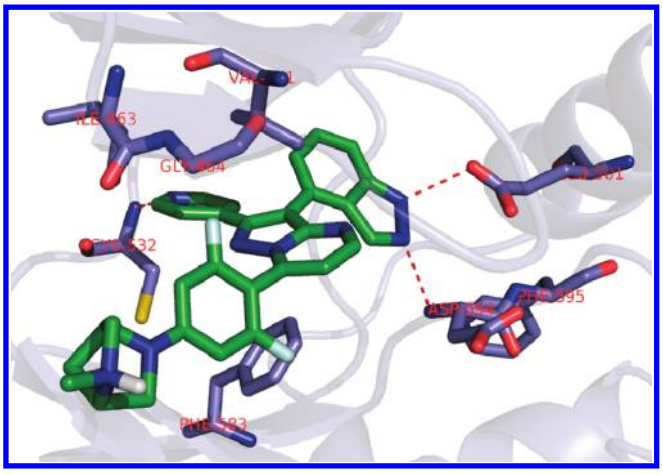

**Figure 2.** Docked model of compound **8l** in the active site of B-Raf.

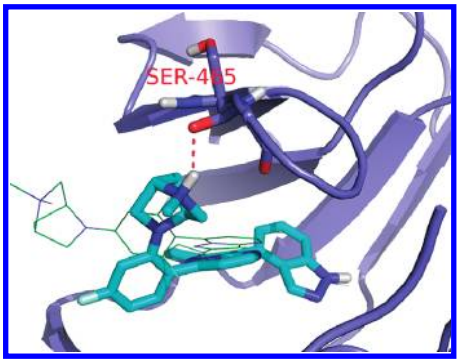


**Figure 3.** Docked model of compound **8o** in the active site of B-Raf (green line represents **8l**).

**Table 2.** Headpiece Modifications of Indazolylpyrazolopyrimidines

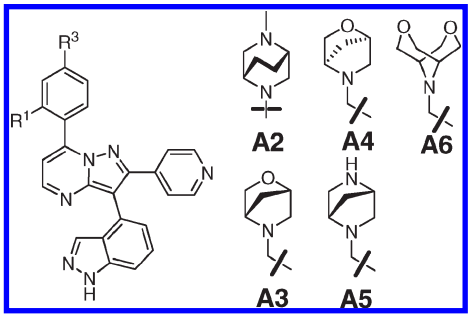


| compd | $R^1$ | $R^3$ | B-Raf $IC_{50}$ (nM) | A375 cell $IC_{50}$ ($\mu$M) |
|---|---|---|---|---|
| **15a** | | **A2** | 0.71 | 0.185 |
| **15b** | F | **A2** | 0.41 | 0.118 |
| **15c** | | **A3** | 10 | 0.945 |
| **15d** | F | **A3** | 1.2 | 0.268 |
| **15e** | F | **A4** | 0.52 | 0.078 |
| **15f** | | **A5** | 2.3 | 9.475 |
| **15g** | F | **A6** | 0.77 | 0.304 |

In an early metabolite identification study with **8b**, significant amounts of desmethylation (**16a**, B-Raf kinase $IC_{50} \leq$ 0.32 nM; A375 $IC_{50}$ = 0.117 $\mu$M) and N-oxidation (**17a**, B-Raf kinase $IC_{50}$ = 0.59 nM; A375 $IC_{50}$ = 2.153 $\mu$M), on the alkylamino nitrogen were observed (see Figure 4). Therefore, a survey of the *N*-alkyl group was performed to test if bulky substituents can block these metabolic pathways. Surprisingly analogues (**18a**−**d**) with large alkyl groups are more labile than the parent methyl compound (Table 3), though all of them showed excellent enzyme activity consistent with what the model predicts. Nevertheless, it was found that **8l** with two ortho fluorine atoms was quite stable in human and nude mouse microsomes and gave very small amounts of these metabolites (**16b**, B-Raf kinase $IC_{50} \leq 0.32$ nM; A375 $IC_{50}$ = 0.020 $\mu$M; **17b**, B-Raf kinase $IC_{50}$ = 17 nM; A375 $IC_{50}$ = 0.229 $\mu$M).

A biomarker study showed that **1b**, **8b**, and **8l** significantly decrease the phosphorylation of downstream ERK kinase in cell culture (Figure 5), which correlated well with the inhibition of cellular proliferation. This result strongly supports that the antitumor activity of these compounds comes from the inhibition of the Raf signaling pathway.

Compound **8l** also possesses a favorable pharmacokinetic profile in nude mice. It has moderate half-life (3.5 h) and clearance (23 (mL/min)/kg) and good exposure ($AUC_{inf}$ = 4000 h·ng/mL, po 10 mg/kg) and bioavailability (54%).

**Scheme 2**[a]

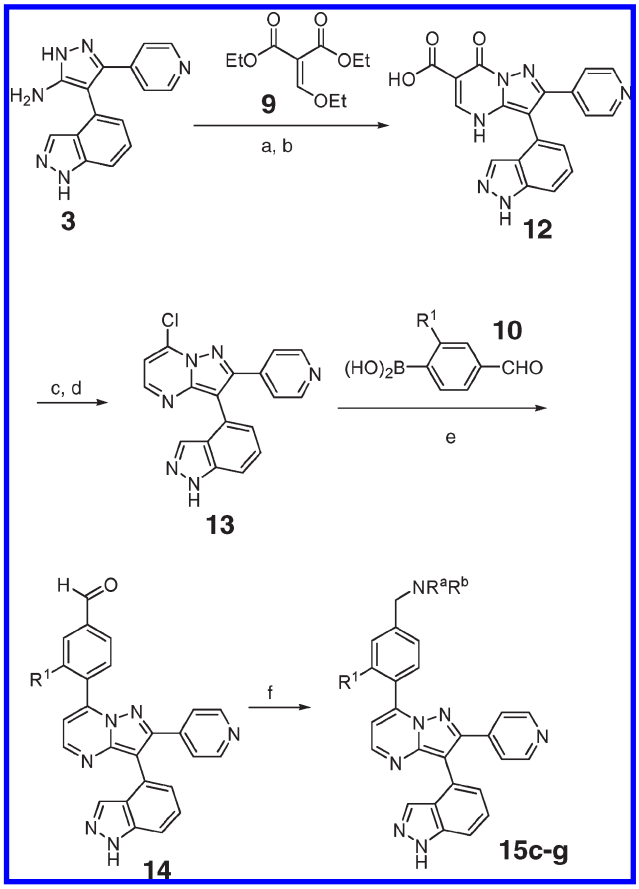


[a] Reagents and conditions: (a) **9**, HOAc, reflux, 55%; (b) 2.5 N NaOH, EtOH, reflux, 4.5 h, 85%; (c) Dowtherm, 245 °C, 90%; (d) $POCl_3$, *N*,*N*-diethylaniline, 100°C; (e) **10**, cat. $PdCl_2$(dppf), $Na_2CO_3$, DME, microwave, 110 °C, 1 h, 43−50%; (f) $R^aR^bNH$, $NaBH(OAc)_3$, HOAc, DMF, room temp, 16 h, 27−58%.

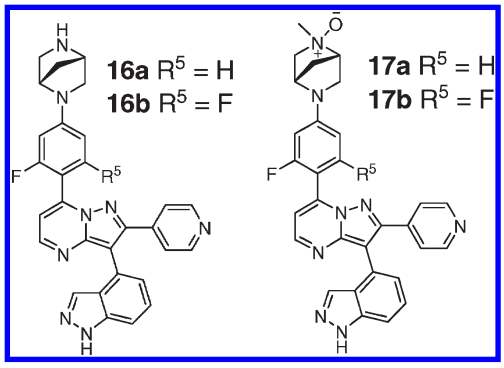


**Figure 4.** Metabolites from **8b** and **8l**.

Moreover, it was also found that **8l** stays in tumor tissue for a long period. The postdose (po 25 mg/kg) tumor concentrations of **8l**[8] were 6.6 and 6.1 $\mu$M after 6 and 24 h, respectively, while the plasma concentration of **8l** was 0.06 $\mu$M after 24 h. A pharmacodynamic study in A375 xenograft mouse model indicated complete ERK phosphorylation inhibition even after 24 h (iv, 50 mg/kg, data not shown). Repeat oral dosing in the A375 mouse resulted in excellent tumor growth inhibition and good suppression of ERK phosphorylation in tumor tissue at 10 mg/kg q.d. (Figure 6). Even at a dose of 7.5 mg/kg q.d. a 39% tumor growth inhibition (TGI) was observed

**Table 3.** *N*-Alkyl Variation of Indazolylpyrazolopyrimidine Analogues

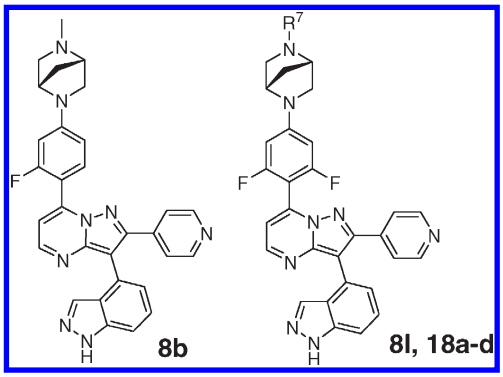


| compd | $R^7$ | B-Raf $IC_{50}$ (nM) | A375 $IC_{50}$ ($\mu$M) | $t_{1/2}$ (min) (human) | $t_{1/2}$ (min) (nude mice) |
|---|---|---|---|---|---|
| **8b** | | 0.23 | 0.044 | 17 | > 30 |
| **8l** | Me | 0.16 | 0.024 | > 30 | > 30 |
| **18a** | Et | < 0.32 | 0.056 | 11 | nd |
| **18b** | *i*-Pr | < 0.32 | 0.055 | 5 | 17 |
| **18c** | *i*-Bu | < 0.32 | 0.089 | 3 | 4 |
| **18d** | cyclobutyl | < 0.32 | 0.078 | 3 | 5 |

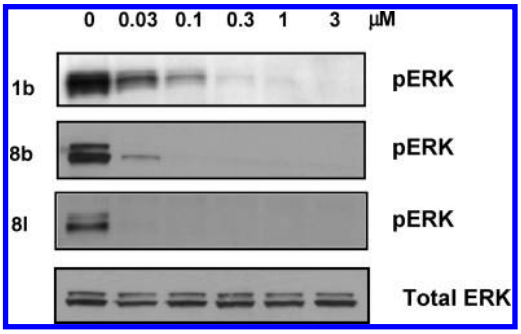


**Figure 5.** Biomarker (pERK) inhibition in A375 cell line.

(data not shown).[9] Although **8l** appeared well tolerated, we are aware that this series of compounds can promote the MAPK pathway in certain B-Raf wild type cell lines,[10] leading to some undesired consequences. This observation has been reported for other B-Raf inhibitors,[3a,c] and an inhibitor induced dimerization/activation mechanism[11] has been proposed to explain it.

## Conclusions

In summary, a novel series of selective B-Raf inhibitors is disclosed. The potency of indazolylpyrazolopyrimidine analogues was optimized through fine-tuning of the substituents on the phenyl linker. The introduction of two ortho fluorine atoms led to the identification of an extremely potent compound **8l**, which also demonstrated potent antitumor activity in the B-Raf mutant xenograft mouse model.[12]

## Experimental Section

**Chemistry.** $^1$H NMR spectra were recorded at 400 MHz with a Bruker DPX-400 spectrometer (unless otherwise noted) at ambient temperature. $^{13}$C NMR spectra were recorded at 100 MHz (unless otherwise noted) at ambient temperature. Chemical shifts were reported in parts per million relative to $CDCl_3$ ($^1$H, $\delta$ 7.24), $CD_3OD$ ($^1$H, $\delta$ 3.31), or DMSO-$d_6$ ($^1$H, $\delta$ 2.50). Data for $^1$H NMR are reported as follows: chemical shift, integration, multiplicity (s = singlet, d = doublet, t = triplet, q = quartet, m = multiplet, br = broad), and coupling constants. All $^{13}$C NMR spectra were recorded with complete proton decoupling. All reactions were carried out in air-dried glassware under a nitrogen atmosphere unless otherwise noted. Unless otherwise noted, reagents were obtained from commercial sources and were used without further purification. All the final products were > 95% pure as determined by HPLC.

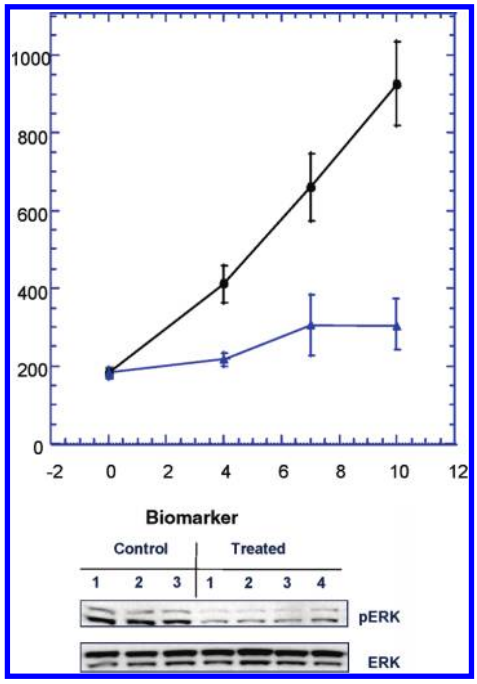


**Figure 6.** A375 xenograft growth inhibition. Compound **8l** was orally dosed at 10 mg/kg once a day. Each arm had $n$ = 10, and tumors were measured with calipers at the designated times. Error bars represent standard deviation, and the results are statistically significant. A375 tumors were harvested from treated and non-treated animals 6 h after an initial oral dose of 10 mg/kg **8l**. Tumor lysates were made and probed by immunoblotting for the presence of pERK and total ERK.

**7-(2,6-Difluoro-4-((1*S*,4*S*)-5-methyl-2,5-diazabicyclo[2.2.1]-heptan-2-yl)phenyl)-3-(1*H*-indazol-4-yl)-2-(pyridin-4-yl)pyrazolo-[1,5-α]pyrimidine (8l). Step 1.** To a solution of 1-(2,4,6-trifluorophenyl)ethanone (**4l**) (3.9 g, 22.5 mmol) in 30 mL of hexamethylphosphoramide, (1*S*,4*S*)-*tert*-butyl 2,5-diazabicyclo[2.2.1]-heptane-2-carboxylate (**2**) (3.0 g, 15 mmol) and potassium carbonate (6.2 g, 45 mmol) were added. This solution was stirred at room temperature for 4 days. The mixture was then diluted with 200 mL of diethyl ether and was washed with 200 mL of water. The aqueous solution was extracted twice with diethyl ether. The combined organic layer was washed with water three times, then dried over anhydrous sodium sulfate, and concentrated. The residue was purified by silica gel chromatography (isopropanol, hexanes) to give (1*S*,4*S*)-*tert*-butyl 5-(4-acetyl-3,5-difluorophenyl)-2,5-diazabicyclo[2.2.1]heptane-2-carboxylate (**5l**) (3.3 g, 62%) as an off-white solid. $^1$H NMR (400 MHz, $CDCl_3$, mixture of rotamers): $\delta$ 6.02 (d, $J$ = 12.4 Hz, 2H), 4.68 (br s, 0.54H), 4.54 (br s, 0.46H), 4.37 (br s, 1H), 3.54−3.14 (m, 4H), 2.52 (t, $J$ = 2.8 Hz, 3H), 2.04−1.92 (m, 2H), 1.47 (br s, 4.1H), 1.43 (br s, 4.9H). $^{13}$C NMR (75 MHz, CDCl3): $\delta$ 193.1, 163.3 (dd, $J$ = 252.0, 10.5 Hz), 154.0, 150.1 (t, $J$ = 14.7 Hz), 105.9 (t, $J$ = 15.6 Hz), 95.2 (d, $J$ = 29.2 Hz), 80.1, 57.9/57.4, 57.0/56.8, 56.5/56.1, 52.2/51.8, 37.7/37.2, 32.5 (t, $J$ = 3.9 Hz), 28.4. HRMS [$(M + H)^+$] calcd for $C_{18}H_{22}F_2N_2O_3$ 353.1670, found 353.1676.

**Step 2.** A mixture of **5l** (3.3 g, 9.4 mmol) and 30 mL of 1, 1-dimethoxy-*N*,*N*-dimethylmethanamine was refluxed for 35 h. The reaction mixture was concentrated and the residue was purified by silica gel chromatography (isopropanol, dichloromethane) to give (1*S*,4*S*)-*tert*-butyl 5-(4-((*E*)-3-(dimethylamino)acryloyl)-3,5-difluorophenyl)-2,5-diazabicyclo[2.2.1]heptane-2-carboxylate (**6l**)

(3.5 g, 90%) as an oil. $^1$H NMR (400 MHz, $CDCl_3$, mixture of rotamers): $\delta$ 7.53 (br, 2H), 6.03 (d, $J$ = 11.2 Hz, 2H), 4.64 (br s, 0.53H), 4.51 (br s, 0.47H), 4.32 (br s, 1H), 3.67−3.33 (m, 4H), 3.10 (s, 3H), 2.87 (s, 3H), 2.01−1.88 (m, 2H), 1.46 (br s, 4.2H), 1.43 (br s, 4.8H). MS [(M + H)$^+$] calcd for $C_{21}H_{28}F_2N_3O_3$ 408.2, found 408.2.

**Step 3.** To a solution of 2,2,2-trifluoroacetic acid (0.54 mL) in 18 mL of methanol, **6l** (1.1 g, 2.6 mmol) and 4-(1*H*-indazol-4-yl)-3-(pyridin-4-yl)-1*H*-pyrazol-5-amine (**3**) (0.72 g, 2.6 mmol) were added. This solution was stirred at room temperature for 7 days (not optimized). The mixture was basified with methanolic ammonia, taken up with silica gel, and purified by silica gel chromatography (isopropanol, dichloromethane) to give (1*S*,4*S*)-*tert*-butyl-5-(4-(3-(1*H*-indazol-4-yl)-2-(pyridin-4-yl)-pyrazolo[1,5-α]pyrimidin-7-yl)-3,5-difluorophenyl)-2,5-diazabicyclo[2.2.1]heptane-2-carboxylate (**7l**) (1.4 g, 87%) as a yellow solid. $^1$H NMR (400 MHz, $CDCl_3$, mixture of rotamers): $\delta$ 8.54 (d, $J$ = 4.4 Hz, 1H), 8.46 (d, $J$ = 6.0 Hz, 2H), 7.72, (s, 1H), 7.56−7.45 (m, 4H), 7.28 (d, $J$ = 2.4 Hz, 1H), 6.99 (d, $J$ = 4.0 Hz, 1H), 6.28 (d, $J$ = 11.6 Hz, 2H), 4.73 (br s, 0.54H), 4.59 (br s, 0.46H), 4.45 (br s, 1H), 3.67−3.22 (m, 4H), 2.10−1.98 (m, 2H), 1.50 (br s, 4.2H), 1.46 (br s, 4.8H). MS [(M + H)$^+$] calcd for $C_{34}H_{30}F_2N_8O_2$ 621.3, found 621.3.

**Step 4.** A solution of **7l** (1.4 g, 2.3 mmol) in 6 N HCl (19 mL of concentrated HCl and 19 mL of methanol) was stirred for 1 h. The mixture was concentrated, basified with methanolic ammonia, taken up with silica gel, and purified by silica gel chromatography (ammonia, methanol, dichloromethane) to give 7-(4-((1*S*,4*S*)-2,5-diazabicyclo[2.2.1]heptan-2-yl)-2,6-difluorophenyl)-3-(1*H*-indazol-4-yl)-2-(pyridin-4-yl)pyrazolo[1,5-α]pyrimidine (**16b**) (1.1 g, 92%) as a yellow solid. $^1$H NMR (400 MHz, $CD_3OD$): $\delta$ 8.55 (d, $J$ = 4.4 Hz, 1H), 8.40−8.37 (m, 2H), 7.64−7.47 (m, 5H), 7.26 (dd, $J$ = 7.2, 0.8 Hz, 1H), 7.17 (d, $J$ = 4.4 Hz, 1H), 6.48 (d, $J$ = 12.0 Hz, 2H), 4.61 (br s, 1H), 4.03 (br s, 1H), 3.65 (dd, $J$ = 9.8, 2.2 1H), 3.32−3.23 (m, 1H), 3.17−3.09 (m, 2H), 2.09 (d, $J$ = 9.6 Hz, 1H), 1.93 (d, $J$ = 10.0 Hz, 1H). MS [(M + H)$^+$] calcd for $C_{29}H_{22}F_2N_8$ 521.2, found 521.3.

**Step 5.** To a solution of **16b** (1.1 g, 2.1 mmol) in 30 mL of DMF, formaldehyde (0.47 mL, 6.3 mmol) and sodium triacetoxyhydroborate (1.3 g, 6.3 mmol) were added. This solution was stirred at room temperature for 2 h and then concentrated on rotavapor. The residue was stirred with 15 mL of 7 N methanolic ammonia overnight. The solution was concentrated and purified with silica gel chromatography (methanol, dichloromethane) to give **8l** (0.95 g, 85%) as a yellow solid. $^1$H NMR (400 MHz, DMSO-$d_6$): $\delta$ 13.21 (s, 1H), 8.63 (d, $J$ = 4.4 Hz, 1H), 8.51−8.46 (m, 2H), 7.59 (d, $J$ = 8.4 Hz, 1H), 7.54 (s, 1H), 7.44 (dd, $J$ = 8.4, 6.8 Hz, 1H), 7.40−7.36 (m, 2H), 7.32 (d, $J$ = 4.4 Hz, 1H), 7.19 (d, $J$ = 7.2 Hz, 1H), 6.58 (d, $J$ = 7.2 Hz, 2H), 4.54 (s, 1H), 4.35 (s, 1H), 3.37−3.31 (m, 2H), 2.83 (dd, $J$ = 9.2, 1.6 Hz, 1H), 2.56−2.50 (m, 1H), 2.32 (s, 3H), 1.92 (d, $J$ = 9.6 Hz, 1H), 1.78 (d, $J$ = 9.2 Hz, 1H); $^{13}$C NMR (100 MHz, DMSO-$d_6$): $\delta$ 161.0 (dd, $J$ = 243.9, 9.7 Hz), 150.1 (t, $J$ = 14.8 Hz), 149.8, 149.6, 149.5, 147.3, 140.10, 140.06, 137.1, 133.5, 126.0, 123.5, 122.4, 122.3, 122.2, 112.2, 109.4, 107.8, 94.8 (d, $J$ = 27.2 Hz), 93.7 (t, $J$ = 20.2 Hz), 62.1, 59.4, 58.3, 52.4, 40.7, 35.2. HRMS [(M + H)$^+$] calcd for $C_{30}H_{24}F_2N_8$ 535.2165, found 535.2158.

**Acknowledgment.** We thank Drs. Tarek Mansour, Robert Abraham, John Ellingboe, Derek Cole, Ariamala Gopalsamy, and Suvit Thaisrivongs for their support of this work.

**Supporting Information Available:** Synthesis details for compounds, spectroscopic data, assay protocols, and kinase selectivity profile of **8l**. This material is available free of charge via the Internet at http://pubs.acs.org.

**Note Added after ASAP Publication.** This paper was published on the web on October 20, 2010 with an error in Figure 1. The revised version was published on November 4, 2010.

## References

(1) Wellbrook, C.; Karasarides, M.; Marais, R. The RAF proteins take centre stage. *Nat. Rev. Mol. Cell Biol.* **2004**, *5*, 875–885.

(2) Davies, H.; Bignell, G. R.; Cox, C.; Stephens, P.; Edkins, S.; Clegg, S.; Teague, J.; Woffendin, H.; Garnett, M. J.; Bottomley, W.; Davis, N.; Dicks, E.; Ewing, R.; Floyd, Y.; Gray, K.; Hall, S.; Hawes, R.; Hughes, J.; Kosmidou, V.; Menzies, A.; Mould, C.; Parker, A.; Stevens, C.; Watt, S.; Hooper, S.; Wilson, R.; Jayatilake, H.; Gusterson, B. A.; Cooper, C.; Shipley, J.; Hargrave, D.; Pritchard-Jones, K.; Maitland, N.; Chenevix-Trench, G.; Riggins, G. J.; Bigner, D. D.; Palmieri, G.; Cossu, A.; Flanagan, A.; Nicholson, A.; Ho, J. W. C.; Leung, S. Y.; Yuen, S. T.; Weber, B. L.; Seigler, H. F.; Darrow, T. L.; Paterson, H.; Marais, R.; Marshall, C. J.; Wooster, R.; Stratton, M. R.; Futreal, P. A. Mutations of the BRAF gene in human cancer. *Nature* **2002**, *417*, 949–954.

(3) Recent examples of B-Raf inhibitors with in vivo efficacy: (a) King, A. J.; Patrick, D. R.; Batorsky, R. S.; Ho, M. L.; Do, H. T.; Zhang, S. Y.; Kumar, R.; Rusnak, D. W.; Takle, A. K.; Wilson, D. M.; Hugger, E; Wang, L.; Karreth, F.; Lougheed, J. C.; Lee, J.; Chau, D.; Stout, T. J.; May, E. W.; Contractor, R. G.; Smalley, K. S. M.; Herlyn, M.; Morrissey, M. M.; Tuveson, D. A.; Huang, P. Demonstration of a genetic therapeutic index for tumors expressing oncogenic BRAF by the kinase inhibitor SB-590885. *Cancer Res.* **2006**, *66*, 11100–11105. (b) Tsai, J.; Lee, J. T.; Wang, W.; Zhang, J.; Cho, H.; Mamo, S.; Bremer, R.; Gillette, S.; Kong, J.; Haass, N. K.; Sproesser, K.; Li, L.; Smalley, K. S. M.; Fong, D.; Zhu, Y.-L.; Marimuthu, A.; Nguyen, H.; Lam, B.; Liu, J.; Cheung, I.; Rice, J.; Suzuki, Y.; Luu, C.; Settachatgul, C.; Shellooe, R.; Cantwell, J.; Kim, S.-H.; Schlessinger, J.; Zhang, K. Y. J.; West, B. L.; Powell, B.; Habets, G.; Zhang, C.; Ibrahim, P. N.; Hirth, P.; Artis, D. R.; Herlyn, M.; Bollag, G. Discovery of a selective inhibitor of oncogenic B-Raf kinase with potent antimelanoma activity. *Proc. Natl. Acad. Sci. U.S.A.* **2008**, *105*, 3041–3046. (c) Smith, A. L.; DeMorin, F. F.; Paras, N. A.; Huang, Qi; Petkus, J. K.; Doherty, E. M.; Nixey, T.; Kim, J. L.; Whittington, D. A.; Epstein, L. F.; Lee, M. R.; Rose, M. J.; Babij, C.; Fernando, M.; Hess, K.; Le, Q.; Beltran, P.; Carnahan, J. Selective inhibitors of the mutant B-Raf pathway: discovery of a potent and orally bioavailable aminoisoquinoline. *J. Med. Chem.* **2009**, *52*, 6189–6192.

(4) Wang, X.; Berger, D. M.; Salaski, E. J.; Torres, N.; Hu, Y.; Levin, J. I.; Powell, D.; Wojciechowicz, D.; Collins, K.; Frommer, E. Discovery of highly potent and selective type I B-Raf kinase inhibitors. *Bioorg. Med. Chem. Lett.* **2009**, *19*, 6571–6574.

(5) A model (active conformation) built from 2FB8 (PDB)[3a] was used.

(6) DiGrandi, M. J.; Berger, D. M.; Hopper, D. W.; Zhang, C.; Dutia, M.; Dunnick, A. L.; Torres, N.; Levin, J. I.; Diamantidis, G.; Zapf, C.; Bloom, J. D.; Hu, Y.; Powell, D.; Wojciechowicz, D.; Collins, K.; Frommer, E. Novel pyrazolopyrimidines as highly potent B-Raf inhibitors. *Bioorg. Med. Chem. Lett.* **2009**, *19*, 6957–6961.

(7) Tested by Invitrogen, B-Raf $IC_{50}$ = 0.28 nM in their assay. See Supporting Information for details.

(8) $V_{SS}$ = 4.7 L/kg.

(9) Another efficacy study with Colo205 model also showed great tumor growth inhibition. See Supporting Information for details.

(10) Data are not shown and will be present elsewhere.

(11) (a) Hatzivassiliou, G.; Song, K.; Yen, I.; Brandhuber, B. J.; Anderson, D. J.; Alvarado, R.; Ludlam, M. C.; Stokoe, D.; Gloor, S. L.; Vigers, G.; Morales, T.; Aliagas, I.; Liu, B.; Siberis, S.; Hoeflich, K. P.; Jaiswal, B. S.; Seshagiri, S.; Koeppen, H.; Belvin, M.; Friedman, L. S.; Malek, S. RAF inhibitors prime wild-type RAF to activate the MAPK pathway and enhance growth. *Nature* **2010**, *464*, 431–435. (b) Heidorn, S. J.; Milagre, C.; Whittaker, S.; Nourry, A.; Niculescu-Duvas, I.; Dhomen, N.; Hussain, J.; Reis-Filho, J.; Springer, C. J.; Pritchard, C.; Marais, R. Kinase-dead BRAF and oncogenic RAS cooperate to drive tumor progression through CRAF. *Cell* **2010**, *140*, 209–221. (c) Poulikakos, P.; Zhang, C.; Bollag, G.; Shokat, K. M.; Rosen, N. RAF inhibitors transactivate RAF dimers and ERK signalling in cells with wild-type BRAF. *Nature* **2010**, *464*, 427–430.

(12) Compound **8l** is inefficacious in tumor cell lines with wild type B-Raf.